Information Engine in a Nonequilibrium Bath

Tushar K. Saha,[1,‡] Jannik Ehrich,[1,2,‡] Momčilo Gavrilov,[1] Susanne Still,[2] David A. Sivak,[1,*] and John Bechhoefer[1,†]
[1]Department of Physics, Simon Fraser University, Burnaby, British Columbia, V5A 1S6 Canada
[2]Department of Physics and Astronomy, University of Hawaii at Mānoa, Honolulu, Hawaii 96822, USA

(Received 30 July 2022; accepted 29 June 2023; published 3 August 2023; corrected 17 November 2023)

Information engines can convert thermal fluctuations of a bath at temperature T into work at rates of order k_BT per relaxation time of the system. We show experimentally that such engines, when in contact with a bath that is out of equilibrium, can extract much more work. We place a heavy, micron-scale bead in a harmonic potential that ratchets up to capture favorable fluctuations. Adding a fluctuating electric field increases work extraction up to ten times, limited only by the strength of the applied field. Our results connect Maxwell's demon with energy harvesting and demonstrate that information engines in nonequilibrium baths can greatly outperform conventional engines.

DOI: 10.1103/PhysRevLett.131.057101

Maxwell's famous thought experiment proposed a way to convert information about thermal fluctuations into energy [1]. Exploring "Maxwell demons" has improved our understanding of the second law of thermodynamics [2,3]. Building them, as "information engines," a concept inspired originally by Szilard's model [4], has allowed tests of the second law applied to mesoscopic length scales [5–10]. The ability of an information engine to extract work from a single heat bath is reconciled with the second law because the cost of sensing fluctuations and exploiting the relevant information equals or exceeds the energy extracted [3,4,11,12].

That information-processing costs compensate for the extracted energy implicitly assumes that the measuring device operates at the same temperature as the engine itself. If the temperature of the engine bath exceeds that of the bath connected to the measuring device, net work can be extracted [13]. But the range of temperatures available for heat baths is small, which limits engine power, even with optimized information processing [14]. For example, the ratio of boiling-water to freezing-water temperatures is $373/273 \approx 1.4$, and the ratio of temperatures in an internal-combustion heat engine is $\lesssim 8$, with practical efficiencies $\lesssim 0.5$ [15].

In this Letter, we show experimentally that this limitation can be overcome by immersing the information engine in a nonequilibrium heat bath. The environment is out of equilibrium at macroscopic scales but has practically unchanged local temperature T. The measuring device of the engine is in contact with an equilibrium heat bath also at temperature T. Such an information engine extracts energy from both thermal and nonequilibrium fluctuations. Similar ideas have been proposed theoretically to take advantage of active fluctuations produced by bacteria swimming in a bath [16] and to increase the output of a Szilard engine [17].

With carefully chosen experimental parameters, our engine can extract work at up to 10 times the maximum rate achievable when connected to an equilibrium bath at temperature T. Moreover, we show that energy extraction is constrained only by practical experimental limits on the nonequilibrium forcing of the external environment. The energy extracted can, in principle, exceed the costs associated with necessary information processing and control by orders of magnitude.

Experimental setup.—The information engine consists of an optically trapped, heavy bead in water that acts as a thermal bath at room temperature T [18]. To force the bath out of equilibrium, a fluctuating electric field is applied via electrodes [19]; see Fig. 1(a). Unlike previous experimental implementations of baths with higher effective temperatures that were based on digitally generated noise [19–22], the fluctuating field here arises from a physical reservoir, the amplified Johnson voltage noise of a resistor at temperature T. Under gravity, the bead fluctuates about a mean position because of thermal and nonequilibrium forces acting on it. For details, see the Supplemental Material [23], Sec. I.

System dynamics.—We model the trapped bead as a spring-mass system [Fig. 1(b)]. The information engine

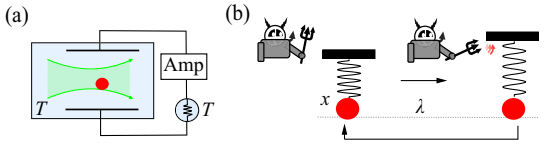

FIG. 1. Schematic of information engine in a nonequilibrium bath. (a) Optically trapped bead in water, subject to nonequilibrium external noise. This external noise is generated by electrodes connected to a resistor in a thermal bath, followed by an amplifier. Both bead and resistor are at room temperature T. (b) Schematic of the information engine.

operates by raising the trap position when the bead fluctuates above the trap center. The upward fluctuation of the bead, increasing its gravitational potential energy, is rectified by ratcheting the trap position. We update the trap position to convert the thermal fluctuations from the nonequilibrium bath into gravitational energy, while ensuring that the shifted trap potential does not perform work on the bead [18].

The position $x(t)$ of a bead trapped in a harmonic potential centered on λ at time t in a nonequilibrium bath is described by the Langevin equation

$$\dot{x}(t) = \underbrace{-[x(t)-\lambda(t)]}_{\text{restoring force}} - \underbrace{\delta_g}_{\text{grav}} + \underbrace{\xi(t)}_{\text{thermal}} + \underbrace{\zeta(t)}_{\text{noneq}}, \quad (1)$$

where lengths are rescaled by the bead position's equilibrium standard deviation $\sigma \equiv \sqrt{k_B T/\kappa}$ in the trap with strength κ and times by the relaxation time $\tau_r \equiv \gamma/\kappa$ of a bead with Stokes' friction coefficient γ in the trap. The scaled effective mass $\delta_g \equiv \Delta m g/(\kappa\sigma)$ accounts for the effects of gravity and buoyancy on a bead with effective mass $\Delta m = \Delta\rho(4/3)\pi r^3$, with r the particle radius and $\Delta\rho$ the density difference between the particle and the surrounding fluid. The noise $\xi(t)$ reflects equilibrium thermal fluctuations of the water bath and is modeled by Gaussian white noise with $\langle \xi(t)\xi(t')\rangle = 2\delta(t-t')$.

We measure the bead position at a sampling time $t_s = 20$ μs. The trap is updated simultaneously with measurements, with a lag of 20 μs. The ratchet feedback algorithm is

$$\lambda_{k+1} = \lambda_k + \alpha\,(x_k - \lambda_k)\Theta(x_k - \lambda_k), \quad (2)$$

for step function $\Theta(\cdot)$ and scalar feedback gain α. When the particle position is accurately known and fluctuations arise from an equilibrium thermal bath, feedback rules of the form of Eq. (2) can extract maximum free energy [18,35,36].

Nonequilibrium bath.—The second noise $\zeta(t)$ in Eq. (1) describes random electrokinetic forcing of strength D_{ne}. The electrokinetic forces combine electro-osmotic and electrophoretic effects on the bead [37]. Here, we empirically determine the nonequilibrium-noise strength.

The fluctuating electrokinetic forces arise from the amplified, low-pass-filtered Johnson noise of a resistor. In scaled units, the noise term obeys

$$f_{ne}^{-1}\dot{\tilde{\zeta}}(t) = -\tilde{\zeta}(t) + \sqrt{D_{ne}}\tilde{\xi}(t), \quad (3)$$

where f_{ne} is the *cutoff* frequency set by the filter frequency, $\langle\tilde{\xi}(t)\rangle = 0$, and $\langle\tilde{\xi}(t)\tilde{\xi}(t')\rangle = 2\delta(t-t')$. The low-pass filter generates exponentially correlated colored nonequilibrium Ornstein-Uhlenbeck noise, $\langle\zeta(t)\zeta(t')\rangle = D_{ne} f_{ne} e^{-f_{ne}|t-t'|}$, which tends to white noise for $f_{ne} \to \infty$. The dynamics of particles subjected to such noise have been studied extensively [22,38–40]. D_{ne} varies from 0 to 83.5 and f_{ne} from 10 Hz to 24 kHz. The trap's cutoff frequency $f_c = 1/(2\pi\tau_r)$ is 200 ± 2 Hz.

Energy measurements.—At each time step, the stored gravitational (free) energy of the bead changes by

$$\Delta F_{k+1} = \delta_g(\lambda_{k+1} - \lambda_k). \quad (4)$$

The average output power is measured using $\dot{F} = \sum_{k=1}^{N}\langle\Delta F_k\rangle/Nt_s$, where $\langle\cdot\rangle$ denotes averaging over multiple trajectories, each of length N time steps.

The work done by the trap on the bead is

$$W_{k+1} = \frac{1}{2}[(x_{k+1} - \lambda_{k+1})^2 - (x_{k+1} - \lambda_k)^2], \quad (5)$$

and the average trap power is measured using $\dot{W} = \sum_{k=1}^{N}\langle W_k\rangle/Nt_s$.

Equation (5) implies that the trap power would be zero for $\alpha = 2$ because the trap is ratcheted such that the particle's potential energy does not change; however, during the one-step delay, the particle on average loses some potential energy [18]. To compensate, the trap should not be moved as far, which is realized by reducing the feedback gain α, empirically to $\alpha \approx 1.8$ when measurement noise is negligible [36].

Results.—We study the dependence of the information engine's output power on the characteristics of the nonequilibrium noise.

First, we measure the output power $\dot{F}$ for different noise cutoff frequencies f_{ne}, at fixed amplitude $D_{ne} = 3.0$. Figure 2(a) shows that the output power increases with

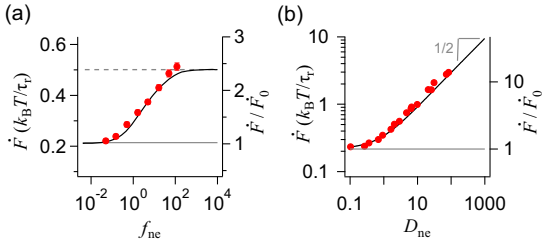

FIG. 2. Output-power optimization for a 3-μm bead at $\alpha = 1.8$. (a) Output power as a function of cutoff frequency f_{ne} of the nonequilibrium bath scaled by the trap cutoff frequency f_c, at nonequilibrium-noise strength $D_{ne} = 3.0$ and scaled mass $\delta_g = 0.37$. Dashed line: high-f_{ne} limit, from Eq. (9). Gray line: measured output power $\dot{F}_0$ at equilibrium ($D_{ne} = 0$). Black curve: prediction based on numerical simulations, using the measured D_{ne}; not a fit. Right axis: ratio of nonequilibrium to equilibrium output powers. (b) Output power as a function of D_{ne} for high cutoff frequency ($f_{ne} = 118$). Gray line: measured output power at $D_{ne} = 0$ and $\delta_g = 0.38$. Black curve: scaling-theory prediction from Eq. (9), showing the asymptotic $\sim D_{ne}^{1/2}$ dependence.

f_{ne}, in agreement with numerical simulations (see Supplemental Material [23], Sec. III). The output power saturates at $f_{ne} \gtrsim 100$: At high f_{ne}, the bead cannot follow the force fluctuations and thus effectively experiences white noise indistinguishable from that of a thermal bath with a higher "effective temperature." Further increases in the cutoff frequency do not affect the bead's dynamics. At low f_{ne}, the nonequilibrium fluctuations are weaker than the equilibrium thermal fluctuations, and the output power equals that in a thermal bath at room temperature. At the maximum f_{ne}, the output power is 2.4× that for a purely thermal bath.

Next, we study the dependence of the output power on the nonequilibrium-noise strength D_{ne} using a variable-gain amplifier. We fix the low-pass filter's cutoff frequency f_{ne} to be ≈100 times that of the trap, so that all experiments are in the limit where the nonequilibrium environment provides effectively white-noise fluctuations to the bead. Figure 2(b) shows that the output power increases with the noise strength D_{ne}. At low D_{ne}, the power is that achievable with a purely thermal bath at room temperature. As D_{ne} is increased, the output power increases monotonically. In our experiments, electrochemical reactions at the electrodes limit the maximum achievable noise strength and hence the output power of the information engine. Maximizing both cutoff frequency f_{ne} and noise strength D_{ne}, we achieve an increase of 14× in output power relative to the equilibrium case, to $3.81.6 \times 10^3 k_B T/\mathrm{s} = 1.6 \times 10^{-17}$ W.

A simple scaling argument in the white-noise limit explains the observed performance increase: In Ref. [18], we found the output power of the purely thermal information engine to be, for $t_s \ll 1$ and with $\dot{F}_0 \equiv \dot{F}(D_{ne} = 0)$,

$$\dot{F}_0 = \sqrt{\frac{2}{\pi}}\delta_g e^{-\delta_g^2/2}\left[1 + \mathrm{erf}\left(\frac{\delta_g}{\sqrt{2}}\right)\right]^{-1}. \quad (6)$$

For $f_{ne} \gg 1$, the exponentially correlated Ornstein-Uhlenbeck noise $\zeta(t)$ in Eq. (3) becomes effectively white noise, relative to the trap's cutoff frequency f_c. In this limit and ignoring inertial and hydrodynamic corrections to the overdamped Langevin dynamics of the bead [41], it makes sense to view the bead as being immersed in a bath with a higher "effective temperature" T_{ne}. Since ξ and $\tilde{\xi}$ are uncorrelated,

$$\left\langle \left[\xi(t) + \sqrt{D_{ne}}\tilde{\xi}(t)\right]\left[\xi(t') + \sqrt{D_{ne}}\tilde{\xi}(t')\right]\right\rangle = 2(1 + D_{ne})\delta(t - t'), \quad (7)$$

and the effective temperature ratio, in physical units, is $T_{ne}/T = 1 + D_{ne}/D$ or, in scaled units, $T_{ne} = 1 + D_{ne}$.

Higher (effective) temperature T_{ne} rescales $\dot{F}_0$ in Eq. (6) and the scaled effective mass $\delta_g \propto T^{-1/2}$. We therefore define

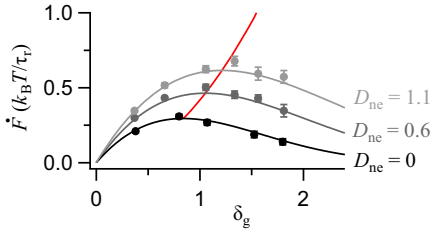

FIG. 3. Optimizing output power as a function of scaled mass δ_g for different nonequilibrium-noise strengths. Markers: experiments; lines: Eq. (9). Red curve parametrically plots maximal $\dot{F}$ and δ_g that maximizes $\dot{F}$ [calculated from Eq. (10)], as functions of D_{ne}.

$$\tilde{\delta}_g(D_{ne}) \coloneqq \frac{\delta_g}{\sqrt{1 + D_{ne}}}. \quad (8)$$

In the white-noise limit, the output power is thus

$$\dot{F} = (1 + D_{ne})\sqrt{\frac{2}{\pi}}\tilde{\delta}_g e^{-\tilde{\delta}_g^2/2}\left[1 + \mathrm{erf}\left(\frac{\tilde{\delta}_g}{\sqrt{2}}\right)\right]^{-1}. \quad (9)$$

Substituting Eq. (8) for $\tilde{\delta}_g$ into Eq. (9) gives, for $D_{ne} \gg 1$, the asymptotic behavior $\dot{F} \sim D_{ne}^{1/2}$ seen in Fig. 2(b).

Finally, we study the dependence of the output power on the scaled mass δ_g. Figure 3 shows that for $D_{ne} = 0$, the output power is maximized at an optimum scaled mass $\delta_g \approx 0.845$ [18]. The optimum arises from a trade-off: having a larger mass increases the gravitational energy gained from a favorable up-fluctuation but reduces the frequency of such fluctuations [18,35].

Figure 3 shows that the optimal mass δ_g increases with the nonequilibrium-noise strength D_{ne}. The nonequilibrium noise increases the amplitude of the bead's fluctuation and makes ratchet events more frequent, thereby shifting the optimal trade-off to higher δ_g. Comparing Eqs. (6) and (9), the maximum output power is achieved for $\tilde{\delta}_g(D_{ne}) \approx 0.845$, and hence, according to Eq. (8), for

$$\delta_g \approx 0.845\sqrt{1 + D_{ne}}. \quad (10)$$

The red curve in Fig. 3 represents the maximum achievable output power for different nonequilibrium-noise strengths D_{ne}, achieved at optimal δ_g.

Measure of performance.—As we have seen, operating an information engine in a nonequilibrium bath with noise strength D_{ne} (and effective temperature T_{ne} in the white-noise limit) can increase output power. At the same time, the measuring device and controller that gather and exploit the information used to power the engine are in contact with an equilibrium bath at temperature T and thus independent of the nonequilibrium driving force D_{ne}.

The minimum additional work needed to run the controller is given by the reduction due to the controller's

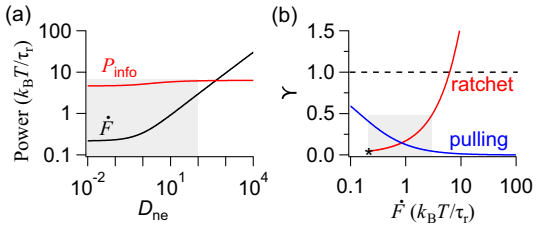

FIG. 4. Numerical estimates of information-engine performance in the white-noise limit ($f_{ne} = 10^4$). (a) Output free-energy gain $\dot{F}$ [Eq. (9)] and information power P_{info} (minimum power to perform measurement, erase information, and control the information engine) as a function of nonequilibrium-noise strength D_{ne}. (b) Measure of performance Υ as a function of $\dot{F}$, compared with a pulling experiment that drags the particle upwards at constant velocity, instead of ratcheting. Star indicates the equilibrium bath, $D_{ne} = 0$. In all calculations, $\delta_g = 0.38$ and $t_s = 1/40$ (experimental parameters). Shaded regions indicate experimentally accessible nonequilibrium-noise strengths.

dynamics in the conditional entropy [24] $H[\Lambda|X]$ of the trap position λ given the particle position x [25]. Therefore, the *information power* required to measure, erase information, and control the engine is

$$P_{info} \equiv \frac{H[\Lambda_{k-1}|X_k] - H[\Lambda_k|X_k]}{t_s}. \tag{11}$$

In the white-noise limit ($f_{ne} \to \infty$), the two conditional entropies can be estimated from simulations and analytical approximations (see Supplemental Material [23], Sec. V). Figure 4(a) compares the input information power P_{info} with the output rate $\dot{F}$ of free-energy gain, Eq. (9), as a function of the noise strength D_{ne}. While the engine output grows as $D_{ne}^{1/2}$, the input power saturates for large D_{ne}, in principle permitting extraction of orders of magnitude more power than required to run the engine, because larger noise strength offers more fluctuations to rectify but does not affect the controller.

The ratio $\Upsilon \equiv \dot{F}/P_{info}$ (power extracted over minimum operating power) is one possible measure of performance. Figure 4(b) shows Υ as a function of the output power $\dot{F}$. With sufficiently strong nonequilibrium fluctuations, output power can exceed input power. In contrast, a "conventional" engine that drags the particle upwards against gravity at the same velocity $v = \dot{F}/\delta_g$ requires trap power $\dot{W} = v^2 + \delta_g v$ and has efficiency < 1 (see Supplemental Material [23], Sec. V.C). This conventional strategy is more efficient at low output power, illustrating that rectifying purely thermal fluctuations is inefficient when using a measuring device and controller that operate at the same temperature. However, with sufficiently strong nonequilibrium fluctuations the information ratchet can extract energy with a lower operating cost. Experimentally, we do not reach the regime of larger output than operating power; however, with the largest experimental noise strengths, the information ratchet requires less operating power than the conventional dragging strategy. Increasing the electric field strengths by using more closely spaced electrodes and more careful choices of electrode material and bath composition could substantially increase the achievable D_{ne} and lead to output powers that exceed minimum information-processing costs.

The quantity Υ has been called an "efficiency" [42,43], as it measures how much of the information acquired by the engine's controller is converted to output work. For the information engines studied in [42,43], the second law requires $\Upsilon \leq 1$ [12,25,42,43]; however, our performance measure does not include the input power delivered by the active process, enabling $\Upsilon > 1$. This is similar to observing a *pseudoefficiency* [44] larger than Carnot efficiency [45–47] in heat engines coupled to active baths. A convenient way to account for the energy input delivered by the active process is to compare the net output power with the rate of effective input "heat" delivered by the combined effects of thermal and nonequilibrium baths in the white-noise limit. An effective *thermal efficiency* defined in this way is lower than the Carnot efficiency of a heat engine working between the controller temperature and the effective bath temperature T_{ne} (see Supplemental Material [23], Sec. V.D), illustrating that the engine does not violate thermodynamic laws.

Discussion and conclusion.—We have shown experimentally that an information engine in contact with a nonequilibrium bath can extract and store an order of magnitude greater power than it can in the same bath without active fluctuations. If the measuring and control devices are at the nominal temperature of the bath (without external forcing) and if the forcing of the nonequilibrium bath is sufficiently strong, then more energy can be extracted than the minimum energy needed to run the measurement-and-control system. Our experiments achieved a performance measure of $\Upsilon = 48.5\%$, limited only by the amount of forcing supplied to the bath.

To understand the significance of these experimental results, we recall that information engines can be connected to two heat baths, a higher-temperature one for the engine itself and a lower-temperature one for the measuring device and controller [13]. This generalized information engine framework was used recently to automate not only the demon's function [4] but also its information processing [13]. Such engines can produce net positive work output and, with optimal information processing, have efficiencies that approach the Carnot limit [14]. Similarly, passive ratchets can extract net work only when connected to heat baths at different temperatures [48–50].

Our information engine extracts energy from only a very small fraction of modes of the high-temperature bath. As Fig. 2(a) shows, an engine need only be supplied with modes slightly exceeding f_c (e.g., $f_{ne} \sim 10^3$ Hz) to achieve

half the maximum possible output. By contrast, equipartition implies that a bath in equilibrium at a temperature T has modes with equal energies up to phonon frequencies, $k_B T/h \approx \mathcal{O}(10^{13})$ Hz, with h Planck's constant [51]. Thus, the fraction of forced modes is only 10^{-10}. Put another way, if the nonequilibrium forcing is removed and the bath returns to equilibrium, its temperature does not measurably increase.

Engines can thus extract work from nonequilibrium modes, while the associated measuring device remains at equilibrium. Given a white-noise spectrum with frequencies 10–100× higher than the engine cutoff frequency, we can assign an effective temperature to the nonequilibrium bath. Because work extraction draws on so few modes, the effective temperature of the bath can be orders of magnitude higher than physical temperatures.

Very high effective temperature and correspondingly large work-extraction rates are implicit in many old technologies: Sailboats move because their sails are constantly adjusted to catch the wind; wind turbines generate power by adjusting their rotors to be normal to the fluctuating wind direction [52]; self-winding watches rectify the nonequilibrium fluctuations supplied by movements of the wearer's arm [50,53]. More recent experimental realizations include ratchets driven by granular gasses [54–58] that achieve effective temperatures $\sim 10^{17}$ K [59–61] and rotors driven by turbulence [62].

Empirically, the scale of the system in many cases is observed to correlate with the power extracted. Our experiments use micron-scale beads and extract powers of $2.97\ k_B T/\tau_r \approx 10^{-17}$ W. For granular media, millimeter-sized beads lead to extracted powers of 10^{-6} W [58]. For wind turbines, the 100-m scale blades lead to extracted powers of 10^6 W [63]. Thus, larger length scales can lead to an increase in the power that can be extracted from a fluctuating environment.

Nonequilibrium fluctuations can also be generated by active media [64–78] such as microswimmer suspensions [79] and active Brownian particles [80]. The huge effective temperatures that one can achieve suggest the potential for drastic efficiency increases. Active cyclically operating heat engines [44–47,81–86] indeed show significant performance increases.

Even in isothermal conditions, the work extracted can exceed the minimum information costs associated with the engine function. We speculate that exploitation of fluctuations, as shown here, could be an organizing principle for molecular machinery, where strong nonequilibrium fluctuations [87,88] speed up various cellular processes [89,90].

Finally, our results also highlight a different way to understand energy harvesting [91–94] by microscopic devices. Such analyses are often specific to the type of systems analyzed. For example, mechanical energy harvesters depend heavily on resonant-forcing mechanisms that make inefficient use of the spectrum of fluctuations [95]. Our approach gives maximum estimates (for a given fluctuation spectrum) of the power that could be extracted and can thus serve as benchmarks for existing systems and may suggest new extraction strategies. The question, which has only begun to be addressed in special cases, is whether "intelligently chosen interventions" [96] can outperform standard passive rectification strategies, such as full-wave rectifier bridge circuits based on diodes or Brownian ratchets [97].

We thank Joseph Lucero and Anand Yethiraj for helpful conversations. This research was supported by grant FQXi-IAF19-02 from the Foundational Questions Institute Fund, a donor-advised fund of the Silicon Valley Community Foundation. Additional support was from grant FQXi-RFP-1820, co-sponsored with the Fetzer Franklin Fund (S. S.), Natural Sciences and Engineering Research Council of Canada (NSERC) Discovery Grants (J. B. and RGPIN-2020-04950 for D. A. S.) and a Tier-II Canada Research Chair CRC-2020-00098 (D. A. S.).

*Corresponding author.
dsivak@sfu.ca
†Corresponding author.
johnb@sfu.ca
‡These authors contributed equally to this work.

[1] J. C. Maxwell, *Theory of Heat*, 3rd ed. (Longmans, Green, and Co., London, 1872).
[2] H. Leff and A. F. Rex, *Maxwell's Demon 2: Entropy, Classical and Quantum Information, Computing* (CRC Press, Florida, 2002).
[3] J. M. Parrondo, J. M. Horowitz, and T. Sagawa, Thermodynamics of information, Nat. Phys. **11**, 131 (2015).
[4] L. Szilard, On the decrease in entropy in a thermodynamic system by the intervention of intelligent beings, in *Maxwell's Demon 2*, edited by H. S. Leff and A. F. Rex (IOP Publishing, Bristol, 2003).
[5] S. Toyabe, T. Sagawa, M. Ueda, E. Muneyuki, and M. Sano, Experimental demonstration of information-to-energy conversion and validation of the generalized Jarzynski equality, Nat. Phys. **6**, 988 (2010).
[6] J. V. Koski, V. F. Maisi, J. P. Pekola, and D. V. Averin, Experimental realization of a Szilard engine with a single electron, Proc. Natl. Acad. Sci. U.S.A. **111**, 13786 (2014).
[7] K. Chida, S. Desai, K. Nishiguchi, and A. Fujiwara, Power generator driven by Maxwell's demon, Nat. Commun. **8**, 15301 (2017).
[8] G. Paneru, D. Y. Lee, T. Tlusty, and H. K. Pak, Lossless Brownian Information Engine, Phys. Rev. Lett. **120**, 020601 (2018).
[9] M. Ribezzi-Crivellari and F. Ritort, Large work extraction and the Landauer limit in a continuous Maxwell demon, Nat. Phys. **15**, 660 (2019).
[10] N. Cottet, S. Jezouin, L. Bretheau, P. Campagne-Ibarcq, Q. Ficheux, J. Anders, A. Auffèves, R. Azouit, P. Rouchon, and

B. Huard, Observing a quantum Maxwell demon at work, Proc. Natl. Acad. Sci. U.S.A. **114**, 7561 (2017).
[11] C. H. Bennett, The thermodynamics of computation—a review, Int. J. Theor. Phys. **21**, 905 (1982).
[12] J. M. Horowitz and H. Sandberg, Second-law-like inequalities with information and their interpretations, New J. Phys. **16**, 125007 (2014).
[13] S. Still, Thermodynamic Cost and Benefit of Memory, Phys. Rev. Lett. **124**, 050601 (2020).
[14] S. Still and D. Daimer, Partially observable Szilard engines, New. J. Phys. **24**, 073031 (2022).
[15] J. Ghojel, *Fundamentals of Heat Transfer* (John Wiley & Sons and ASME Press, New York, 2020).
[16] G. Paneru, S. Dutta, and H. K. Pak, Colossal power extraction from active cyclic Brownian information engines, J. Phys. Chem. Lett. **13**, 6912 (2022).
[17] P. Malgaretti and H. Stark, Szilard Engines and Information-Based Work Extraction for Active Systems, Phys. Rev. Lett. **129**, 228005 (2022).
[18] T. K. Saha, J. N. E. Lucero, J. Ehrich, D. A. Sivak, and J. Bechhoefer, Maximizing power and velocity of an information engine, Proc. Natl. Acad. Sci. U.S.A. **118**, e2023356118 (2021).
[19] I. A. Martínez, E. Roldan, J. M. R. Parrondo, and D. Petrov, Effective heating to several thousand kelvins of an optically trapped sphere in a liquid, Phys. Rev. E **87**, 032159 (2013).
[20] M. Chupeau, B. Besga, D. Guéry-Odelin, E. Trizac, A. Petrosyan, and S. Ciliberto, Thermal bath engineering for swift equilibration, Phys. Rev. E **98**, 010104(R) (2018).
[21] A. Militaru, A. Lasanta, M. Frimmer, L. L. Bonilla, L. Novotny, and R. A. Rica, Kovacs Memory Effect with an Optically Levitated Nanoparticle, Phys. Rev. Lett. **127**, 130603 (2021).
[22] R. Goerlich, L. B. Pires, G. Manfredi, P.-A. Hervieux, and C. Genet, Harvesting information to control non-equilibrium states of active matter, Phys. Rev. E **106**, 054617 (2022).
[23] See Supplemental Material at http://link.aps.org/supplemental/10.1103/PhysRevLett.131.057101, which includes Refs. [18,24–34], for more discussion of the experimental setup and information efficiency.
[24] T. M. Cover and J. A. Thomas, *Elements of Information Theory*, 2nd ed. (Wiley-Interscience, Hoboken, NJ, 2006).
[25] J. Ehrich, S. Still, and D. A. Sivak, Energetic cost of feedback control, Phys. Rev. Res. **5**, 023080 (2023).
[26] A. Kumar and J. Bechhoefer, Nanoscale virtual potentials using optical tweezers, Appl. Phys. Lett. **113**, 183702 (2018).
[27] K. Berg-Sørensen and H. Flyvbjerg, Power spectrum analysis for optical tweezers, Rev. Sci. Instrum. **75**, 594 (2004).
[28] J. Ma, T. Stangner, and F. Kremer, Frequency dependence of the electrophoretic mobility for single colloids as measured using optical tweezers, Phys. Rev. Fluids **2**, 104306 (2017).
[29] T. M. Squires and M. Z. Bazant, Induced-charge electro-osmosis, J. Fluid Mech. **509**, 217 (2004).
[30] D. H. Wolpert, A. Kolchinsky, and J. A. Owen, A space–time tradeoff for implementing a function with master equation dynamics, Nat. Commun. **10**, 1727 (2019).
[31] W. S. Bialek, *Biophysics: Searching for Principles* (Princeton University Press, Princeton, NJ, 2012).
[32] A. Kraskov, H. Stögbauer, and P. Grassberger, Estimating mutual information, Phys. Rev. E **69**, 066138 (2004).
[33] I. A. Martínez, E. Roldán, L. Dinis, D. Petrov, J. M. R. Parrondo, and R. A. Rica, Brownian Carnot engine, Nat. Phys. **12**, 67 (2016).
[34] J. Ehrich, https://github.com/JannikEhrich/Information_engine_in_a_nonequilibrium_bath (2022).
[35] J. N. E. Lucero, J. Ehrich, J. Bechhoefer, and D. A. Sivak, Maximal fluctuation exploitation in Gaussian information engines, Phys. Rev. E **104**, 044122 (2021).
[36] T. K. Saha, J. N. E. Lucero, J. Ehrich, D. A. Sivak, and J. Bechhoefer, Bayesian Information Engine that Optimally Exploits Noisy Measurements, Phys. Rev. Lett. **129**, 130601 (2022).
[37] A. E. Cohen, Trapping and manipulating single molecules in solution, Ph.D. thesis, Stanford University, 2006.
[38] P. Hänggi and P. Jung, Colored noise in dynamical systems, Adv. Chem. Phys. **89**, 239 (1995).
[39] G. Szamel, Self-propelled particle in an external potential: Existence of an effective temperature, Phys. Rev. E **90**, 012111 (2014).
[40] A. Ghosh and A. J. Spakowitz, Statistical behavior of nonequilibrium and living biological systems subjected to active and thermal fluctuations, Phys. Rev. E **105**, 014415 (2022).
[41] T. Franosch, M. Grimm, M. Belushkin, F. M. Mor, G. Foffi, L. Forró, and S. Jeney, Resonances arising from hydrodynamic memory in Brownian motion, Nature (London) **478**, 85 (2011).
[42] M. Bauer, D. Abreu, and U. Seifert, Efficiency of a Brownian information machine, J. Phys. A **45**, 162001 (2012).
[43] H. Sandberg, J.-C. Delvenne, N. J. Newton, and S. K. Mitter, Maximum work extraction and implementation costs for nonequilibrium Maxwell's demons, Phys. Rev. E **90**, 042119 (2014).
[44] A. Datta, P. Pietzonka, and A. C. Barato, Second Law for Active Heat Engines, Phys. Rev. X **12**, 031034 (2022).
[45] S. Krishnamurthy, S. Ghosh, D. Chatterji, R. Ganapathy, and A. K. Sood, A micrometre-sized heat engine operating between bacterial reservoirs, Nat. Phys. **12**, 1134 (2016).
[46] R. Zakine, A. Solon, T. Gingrich, and F. von Wijland, Stochastic Stirling engine operating in contact with active baths, Entropy **19**, 193 (2017).
[47] J. S. Lee, J.-M. Park, and H. Park, Brownian heat engine with active reservoirs, Phys. Rev. E **102**, 032116 (2020).
[48] M. Smoluchowski, Experimentell nachweisbare, der üblichen Thermodynamik widersprechende Molekularphänomene, Phys. Z. **13**, 1069 (1912).
[49] R. P. Feynman, R. B. Leighton, and M. Sands, *The Feynman Lectures on Physics* (Addison-Wesley, Reading, MA, 1963), pp. 46.1–46.9.
[50] J. M. R. Parrondo and P. Español, Criticism of Feynman's analysis of the ratchet as an engine, Am. J. Phys. **64**, 1125 (1996).
[51] H. Nyquist, Thermal agitation of electric charge in conductors, Phys. Rev. **32**, 110 (1928).

[52] G. Stavrakakis, Electrical parts of wind turbines, in *Comprehensive Renewable Energy*, edited by A. Sayigh (Elsevier, New York, 2012).
[53] R. Watkins, *The Origins of Self-Winding Watches 1773–1779*, 2nd ed. (NewPrint, Huntington, Tasmania, 2016).
[54] P. Eshuis, K. van der Weele, D. Lohse, and D. van der Meer, Experimental Realization of a Rotational Ratchet in a Granular Gas, Phys. Rev. Lett. **104**, 248001 (2010).
[55] S. Joubaud, D. Lohse, and D. van der Meer, Fluctuation Theorems for an Asymmetric Rotor in a Granular Gas, Phys. Rev. Lett. **108**, 210604 (2012).
[56] A. Gnoli, A. Petri, F. Dalton, G. Pontuale, G. Gradenigo, A. Sarracino, and A. Puglisi, Brownian Ratchet in a Thermal Bath Driven by Coulomb Friction, Phys. Rev. Lett. **110**, 120601 (2013).
[57] A. Gnoli, A. Sarracino, A. Puglisi, and A. Petri, Nonequilibrium fluctuations in a frictional granular motor: Experiments and kinetic theory, Phys. Rev. E **87**, 052209 (2013).
[58] M. Lagoin, C. Crauste-Thibierge, and A. Naert, Human-Scale Brownian Ratchet: A Historical Thought Experiment, Phys. Rev. Lett. **129**, 120606 (2022).
[59] F. Rouyer and N. Menon, Velocity Fluctuations in a Homogeneous 2d Granular Gas in Steady State, Phys. Rev. Lett. **85**, 3676 (2000).
[60] K. Feitosa and N. Menon, Fluidized Granular Medium as an Instance of the Fluctuation Theorem, Phys. Rev. Lett. **92**, 164301 (2004).
[61] J.-Y. Chastaing, J.-C. Géminard, and A. Naert, Two methods to measure granular gas temperature, J. Stat. Mech. (2017) 073212.
[62] N. Francois, H. Xia, H. Punzmann, and M. Shats, Nonequilibrium Thermodynamics of Turbulence-Driven Rotors, Phys. Rev. Lett. **124**, 254501 (2020).
[63] S. Mathew and G. S. Philip, Wind turbines: Evolution, basic principles, and classifications, in *Comprehensive Renewable Energy*, edited by A. Sayigh (Elsevier, New York, 2012).
[64] S. Ramaswamy, The mechanics and statistics of active matter, Annu. Rev. Condens. Matter Phys. **1**, 323 (2010).
[65] M. C. Marchetti, J. F. Joanny, S. Ramaswamy, T. B. Liverpool, J. Prost, M. Rao, and R. A. Simha, Hydrodynamics of soft active matter, Rev. Mod. Phys. **85**, 1143 (2013).
[66] A. Sokolov, M. M. Apodaca, B. A. Gryzbowski, and I. S. Aranson, Swimming bacteria power microscopic gears, Proc. Natl. Acad. Sci. U.S.A. **107**, 969 (2010).
[67] R. Di Leonardo, L. Angelani, D. Dell'Arciprete, G. Ruocco, V. Iebba, S. Schippa, M. P. Conte, F. Mecarini, F. De Angelis, and E. Di Fabrizio, Bacterial ratchet motors, Proc. Natl. Acad. Sci. U.S.A. **107**, 9541 (2010).
[68] C. J. Olson Reichhardt and C. Reichhardt, Ratchet effects in active matter systems, Annu. Rev. Condens. Matter Phys. **8**, 51 (2017).
[69] G. Vizsnyiczai, G. Fangipane, C. Maggi, F. Saglimbeni, S. Bianchi, and R. Di Leonardo, Light controlled 3D micromotors powered by bacteria, Nat. Commun. **8**, 15974 (2017).
[70] P. Pietzonka, E. Fodor, C. Lohrmann, M. E. Cates, and U. Seifert, Autonomous Engines Driven by Active Matter: Energetics and Design Principles, Phys. Rev. X **9**, 041032 (2019).
[71] E. Fodor and M. E. Cates, Active engines: Thermodynamics moves forward, Europhys. Lett. **134**, 10003 (2021).
[72] T. Speck, Stochastic thermodynamics for active matter, Europhys. Lett. **114**, 30006 (2016).
[73] E. Fodor, C. Nardini, M. E. Cates, J. Tailleur, P. Visco, and F. van Wijland, How Far from Equilibrium is Active Matter?, Phys. Rev. Lett. **117**, 038103 (2016).
[74] D. Mandal, K. Klymko, and M. R. DeWeese, Entropy Production and Fluctuation Theorems for Active Matter, Phys. Rev. Lett. **119**, 258001 (2017).
[75] P. Pietzonka and U. Seifert, Entropy production of active particles and for particles in active baths, J. Phys. A **51**, 01LT01 (2018).
[76] L. Dabelow, S. Bo, and R. Eichhorn, Irreversibility in Active Matter Systems: Fluctuation Theorem and Mutual Information, Phys. Rev. X **9**, 021009 (2019).
[77] L. Caprini, U. M. B. Marconi, A. Puglisi, and A. Vulpiani, The entropy production of Ornstein–Uhlenbeck active particles: A path integral method for correlations, J. Stat. Mech. (2019) 053203.
[78] L. Dabelow and R. Eichhorn, Irreversibility in active matter: General framework for active Ornstein-Uhlenbeck particles, Front. Phys. **8**, 582992 (2021).
[79] J. Elgeti, R. Winkler, and G. Gompper, Physics of microswimmers—single particle motion and collective behavior: A review, Rep. Prog. Phys. **78**, 056601 (2015).
[80] C. Bechinger, R. Di Leonardo, H. Löwen, C. Reichhardt, G. Volpe, and G. Volpe, Active particles in complex and crowded environments, Rev. Mod. Phys. **88**, 045006 (2016).
[81] A. Saha and R. Marathe, Stochastic work extraction in a colloidal heat engine in the presence of colored noise, J. Stat. Mech. (2019) 094012.
[82] A. Kumari, P. S. Pal, A. Saha, and S. Lahiri, Stochastic heat engine using an active particle, Phys. Rev. E **101**, 032109 (2020).
[83] T. Ekeh, M. E. Cates, and E. Fodor, Thermodynamic cycles with active matter, Phys. Rev. E **102**, 010101(R) (2020).
[84] V. Holubec, S. Steffenoni, G. Falasco, and K. Kroy, Active Brownian heat engines, Phys. Rev. Res. **2**, 043262 (2020).
[85] G. Gronchi and A. Puglisi, Optimization of an active heat engine, Phys. Rev. E **103**, 052134 (2020).
[86] N. Roy, N. Leroux, A. K. Sood, and R. Ganapathy, Tuning the performance of a micrometer-sized Stirling engine through reservoir engineering, Nat. Commun. **12**, 4927 (2021).
[87] D. Mizuno, C. Tardin, C. F. Schmidt, and F. C. MacKintosh, Nonequilibrium mechanics of active cytoskeletal networks, Science **315**, 370 (2007).
[88] F. Gallet, D. Arcizet, P. Bohec, and A. Richert, Power spectrum of out-of-equilibrium forces in living cells: Amplitude and frequency dependence, Soft Matter **5**, 2947 (2009).
[89] T. Ariga, K. Tateishi, M. Tomishige, and D. Mizuno, Noise-Induced Acceleration of Single Molecule Kinesin-1, Phys. Rev. Lett. **127**, 178101 (2021).
[90] A. K. Tripathi, T. Das, G. Paneru, G. K. Pak, and T. Tlusty, Acceleration of enzymatic catalysis by active hydrodynamic fluctuations, Commun. Phys. **8**, 101 (2022).

[91] S. P. Beeby, M. J. Tudor, and N. M. White, Energy harvesting vibration sources for microsystems applications, Meas. Sci. Technol. **17**, R175 (2006).
[92] S. Priya, Advances in energy harvesting using low profile piezoelectric transducers, J. Electroceram. **19**, 165 (2007).
[93] K. A. Cook-Chennault, N. Thambi, and A. M. Sastry, Powering MEMS portable devices—a review of non-regenerative and regenerative power supply systems with special emphasis on piezoelectric energy harvesting systems, Smart Mater. Struct. **17**, 043001 (2008).
[94] P. D. Mitcheson, E. M. Yeatman, G. K. Rao, A. S. Holmes, and T. C. Green, Energy harvesting from human and machine motion for wireless electronic devices, Proc. IEEE **96**, 1457 (2008).
[95] L. Gammaitoni, H. Vocca, I. Neri, F. Travasso, and F. Orfei, Vibration energy harvesting: Linear and nonlinear oscillator approaches, in *Sustainable Energy Harvesting Technologies—Past, Present and Future*, edited by T. Y. Kheng (IntechOpen, London, 2011), Chap. 7.
[96] F. Liu, Y. Zhang, O. Dahlsten, and F. Wang, Intelligently chosen interventions have potential to outperform the diode bridge in power conditioning, Nat. Sci. Rep. Ochanomizu Univ. **9**, 8994 (2019).
[97] B. J. Lopez, N. J. Kuwada, E. M. Craig, B. R. Long, and H. Linke, Realization of a Feedback Controlled Flashing Ratchet, Phys. Rev. Lett. **101**, 220601 (2008).

Correction: The author list in Ref. [81] was incorrect and has been fixed.